Environmental Science Nano

Accepted Manuscript

ROYAL SOCIETY OF CHEMISTRY

rsc.li/es-nano

Nano impact

An increasing worldwide attention has been paid to the oil industry pollution especially the frequent occurrence of oil spill. This calls for the environmentally friendly, renewable and effective absorbent materials. The current study explores the effects of carbon nanotubes (CNTs) on the structures, morphologies, specific surface areas and hydrophobic properties of 3D graphene aerogels (GA). The obtained ultra-light graphene-CNTs hybrid aerogels exhibited excellent adsorption capacity to oil and dyes as well as reusability. The present work suggests the promising widespread applications of such hybrid aerogel in the practical water purification and oil remediation.

The ultra-light graphene-CNTs aerogels were successfully synthesized by one-step hydrothermal method and exhibited excellent adsorption capacity to oil and dyes as well as reusability.

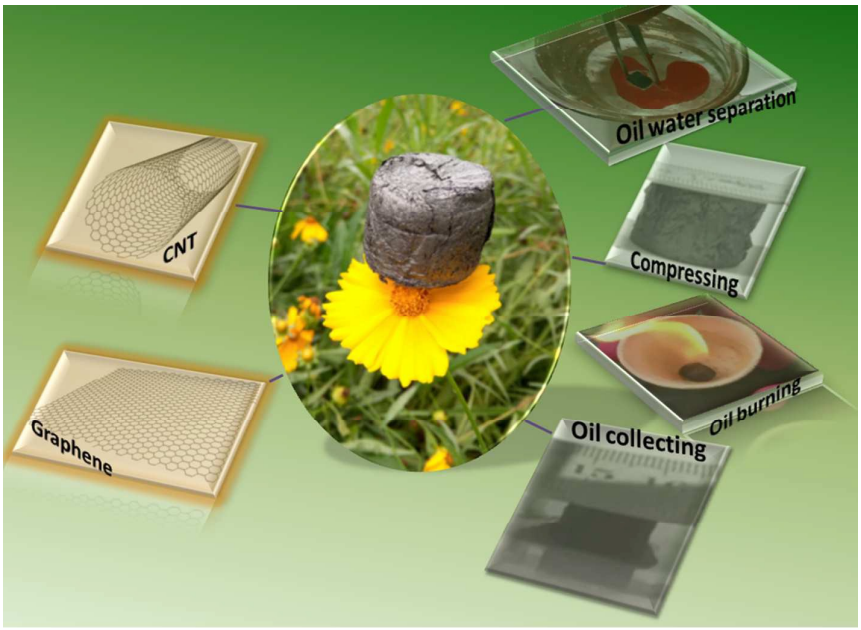

Journal Name

ARTICLE

Graphene-carbon nanotube aerogel as an ultra-light, compressible and recyclable highly efficient absorbent for oil and dyes†

Received 00th January 20xx,
Accepted 00th January 20xx

DOI: 10.1039/x0xx00000x

www.rsc.org/

Wenchao Wan,[a,b] Ruiyang Zhang,[b] Wei Li,[b] Hao Liu,[c] Yuanhua Lin,[a,b] Lina Li,[d] and Ying Zhou[a,b*]

Carbon nanotubes (CNTs) have good toughness and hydrophobicity. The embedding of CNTs into the graphene aerogel (GA) network could modify various properties of the GA. In this work, we report a facile and green approach to synthesize graphene-CNTs aerogel (GCA) by one-step hydrothermal redox reaction. The prepared aerogels possess ultra-light density ranging from 6.2-12.8 mg/cm^3. The incorporation of CNTs into GA could not only improve the morphologies, specific surface areas and hydrophobic properties but also enhance the adsorption capacity and mechanical properties of GA. Under the optimized GO/CNTs mass ratio (7:1 and 3:1) conditions, the adsorption capacity could achieve 100-270 times of its own weight depending on the density of the adsorbed organics. The same trend also appeared in the adsorption of dyes including methyl blue (MB) and methyl orange (MO). Especially, the obtained GCA exhibited excellent reusability and mechanical strength on the basis of absorption-combustion and absorption-squeezing experiments. Even after 10 cycles, the macroscopic shape of the aerogels is well kept and almost no adsorption capacity decreasing was observed. Based on the facile preparation process, high adsorption capacity and stable cyclic performances, the GCA could have promising widespread applications in the practical water purification and oil remediation.

1. Introduction

With the rapid development of economy, the increasing attention has been paid to the severe ecological and environmental problems. Among them, oil industry pollution has been a serious threat to the survival of human beings. In recent years, the frequent occurrence of oil spill has caused immeasurable loss to our living environment and economic development.[1] For instance, in May 2010, the Gulf of Mexico oil spill had caused about 2000 square miles of contaminated areas and billions of dollars pecuniary loss.[2] Recently, adsorption has been considered as one of the most efficient and cost effective methods for oil remediation, but conventional absorbents, such as various inorganic absorbents, natural organic fibres and synthetic organic polymers, tend to suffer from secondary pollution, poor selectivity and low adsorption capacity.[3] Therefore, environmentally friendly, renewable and effective absorbent materials are urgently demanded to deal with the oil spill accident.

Two-dimensional (2D) graphene with one atom thickness, a single layer of graphite, has attracted worldwide attention in recent years due to its excellent physical properties such as high specific surface area, ultra-low density and super hydrophobic.[4] Recent studies revealed that it could be applied as an excellent potential material to deal with the oil contamination and adsorption problems.[5] Nevertheless, 2D graphene film has poor stability, low porosity and collection efficiency, which encountered many obstacles for adsorption of contaminants.[6] Consequently, hierarchical 3D architectures GA through self-assembly processes has been proposed to overcome the limitations of 2D graphene.[7] The GA cannot only maintain the original properties of graphene, but also possess additional advantages such as high porosity and high surface area. The adsorption capacity (Q_{wt}) of GA can be up to several hundred, which is much higher than that of current commercial materials such as sponge, active carbon, wool fiber and zeolite.[8] In addition, other 3D porous structures including CNTs sponges, graphene sponges, CNTs-graphene aerogel, carbonaceous nanofiber aerogels and polydimethylsiloxane (PDMS) sponges also received a great concern.[9] Among them, CNTs and graphene are especially attractive because of their high adsorption capacity, reusability and environmentally friendly.

[a] State Key Laboratory of Oil and Gas Reservoir Geology and Exploitation, Southwest Petroleum University, Chengdu 610500, China. E-mail: yzhou@swpu.edu.cn
[b] The Center of New Energy Materials and Technology, School of Materials Science and Engineering, Southwest Petroleum University, Chengdu 610500, China
[c] Chengdu Green Energy and Green Manufacturing Technology R&D Center, Chengdu 610207, China.
[d] Shanghai Synchrotron Radiation Facility, Shanghai Institute of Applied Physics, Chinese Academy of Sciences, Shanghai 201204, China

† Footnotes relating to the title and/or authors should appear here.
Electronic Supplementary Information (ESI) available: [SEM, TEM images and FT-IR spectra of GCA, the schematic diagram of mechanical compression of GCA; movie for mechanical strength test, movie for adsorption-combustion test, movie for adsorption-squeezing test]. See DOI: 10.1039/x0xx00000x

Generally, both CNTs and graphene have good toughness and high strength,[9d] but the neat graphene and CNTs aerogels have weak elasticity.[10] Recently, the combination of CNTs and graphene to prepare 3D composite aerogels for oil adsorption has been aroused great attention. For example, Gao et al. reported a "sol-cryo" method to synthesize the carbon aerogels with the density of 0.16 mg/cm^3 and these aerogels exhibited excellent mechanical properties. Besides, the adsorption capacity to crude oil can reach as high as 290 g g^{-1}. Nevertheless, this protocol needs to use virulent hydrazine vapor as a deoxidizer, which is harmful for our environment.[11] To overcome this drawback, Losic's group have developed a green and one-step approach using ferrous ions as the green reducing agent to fabricate GCA under hydrothermal conditions.[12] The obtained GCA were able to absorb oils with 21-35 g g^{-1} depending on the density of the adsorbed organics. Although this material reveals a good performance based on continuous vacuum assisted adsorption experiments, the reduced iron nanoparticles on the graphene sheets increased the density of the aerogels. Thus, the adsorption capacity of this material was greatly reduced. Moreover, the mechanical strength of this aerogel was indistinct in this work.[12] Therefore, the quest for the green and facile route to synthesize the ultra-light, high adsorption and mechanical strength GCA is still a tremendous challenge.

In this paper, we report a facile and green approach to synthesize GCA through one-step hydrothermal redox reaction. The obtained aerogels possess ultra-light density ranging from 6.2-12.8 mg/cm^3 depending on the original concentration of GO and CNTs solution. The effects of the amounts of CNTs on the structures, morphologies, specific surface areas, hydrophobic properties, adsorption capacity as well as mechanical properties of GA were investigated systematically. The incorporating of CNTs into the GA cannot only enhance the adsorption capacity but also improve their mechanical properties. Therefore, the obtained GCA with optimizing GO/CNTs ratio exhibited excellent reusability and mechanical strength on the basis of absorption-distillation and absorption-combustion experiments, which are very important for practical water purification and oil remediation applications.

2. Experimental

2.1 Materials

Graphite powder (average lateral size of 500 μm) was purchased from Qingdao Jin Ri Lai Graphite Co., Ltd. Ethylenediamine (EDA), H_2SO_4 (98 %), $KMnO_4$, P_2O_5, H_2O_2 (30 %), $K_2S_2O_8$ and ethanol were purchased from Chengdu Kelong Chemical Co., Ltd. CNTs with the diameter of 40-60 nm were obtained from Shenzhen nano port. High-purity milli-Q water was used in all experiments.

2.2 Preparation of GO

GO was prepared through the oxidation of natural graphite according to a previous reported method.[13] Firstly, the natural graphite flakes (5 g) was added gradually into a 1:3 mixture of fuming nitric acid and sulfuric acid (200 mL). The mixture was magnetic stirring at room temperature for 24 h and then 1 L water was added slowly into the mixture to collect the solids after filtration. The solid products were washed with water and dried at 60 ^{o}C. Then, the dried powders were transferred into an oven at 1000 ^{o}C for ca. 10 s. After that, 5 g of powders, 300 mL of sulfuric acid, 4.2 g $K_2S_2O_8$ and 6.2 g P_2O_5 were successively added into a flask and the mixture was kept at 80 ^{o}C for 5 h. After cooling to room temperature, 2 L water was poured slowly into the mixture, filtered and washed with water using a 0.22 μm pore polycarbonate membrane. The obtained solids were dried in air at room temperature. After that, the solids were added into 200 mL concentrated H_2SO_4 at 0 ^{o}C, then 15 g $KMnO_4$ was added slowly (about 1 h) under continuous stirring condition. After that, the mixture was heated to 35 ^{o}C and stirred for 2 h. The mixture was then diluted with 2 L water, followed through the addition of 10 mL H_2O_2. The mixture was deposited for 2 days and then the upper clarified liquid was removed. The precipitates were washed with water and 1 M HCl. Finally, the washed solution was calibrated (2.5 mg/ml) for further experiments.

2.3 Preparation of GA and GCA

In a typical procedure, a certain amount of CNTs (75 mg) and 0.75 mg polyvinylpyrrolidone (PVP) were added into 30 mL ethanol and the resulting mixture was sonicated for 5 h to form a dispersion (2.5 mg/ml).[14] GO and CNTs solution with different mass ratio including 1:0, 10:1, 7:1, 3:1 and 5:3 with total volume of 40 mL were mixed and stirred for 1 h to form a uniform GO-CNTs dispersion. After that, 160 μL EDA was added and this dispersion was transferred into a Teflon-lined stainless steel autoclave and heated at 120 ^{o}C for 12 h to prepare graphene-CNTs hybrid hydrogel. The resulted hydrogel was washed with high-purity milli-Q water for several times and freeze-dried (-80 ^{o}C pre-cooling) 48 h to obtain the GA and GCA.

2.4 Characterizations

Powder X-ray diffraction (PXRD) was performed through a PANalytical X'pert diffractometer operated at 40 kV and 40 mA using Cu K_α radiation. The Raman spectra of the samples were analyzed on the micro-Raman 2000 system. Scanning electron microscopy (SEM) was performed on a Hitachi S-4800 microscope. Transmission electron microscopy (TEM) was recorded on a FEI Tecnai G2 20 microscope operated at 200 kV. The Fourier transform infrared (FT-IR) spectra were recorded on a Nicolet 6700 spectrometer. The contact angle was tested by the JY-82C video contact angle tester. The specific surface area (SSA) was determined through the adsorption of methylene blue (MB) method by UV-vis spectroscopy (Shimadzu UV-2600).[15] The SSA of the aerogels was calculated using the following equation:

$$SSA = \frac{N_A A_{MB} (C_0 - C_e)V}{M_{MB}\, m_s}$$

where N_A is Avogadro number (6.02×10^{23} mol^{-1}), A_{MB} is the covered area of per MB molecule (typically assumed to be 1.35 nm^2), C_0 and C_e are the initial and equilibrium concentrations of MB, respectively, V is the volume of MB solution, M_{MB} is the relative molecular mass of MB, and m_s is the mass of the sample.

2.5 Adsorption capacity measurements

For the oil-water adsorption tests, firstly, toluene was stained by the sudan red and then 2 mL of stained toluene was added into the water. 5.8 mg of the prepared aerogel was put into this solution. The adsorbents were removed after the oil or organic was

completely adsorbed. To investigate the adsorption performances of the GCA, oil (lube), polar organics (n-hexane, ethanol and toluene) and non-polar organics (phenixin) were selected for measurements. The weight of the GCA adsorbents was recorded before immersing in the oil. The adsorbents were weighed again after about 5 min of immersing. The adsorption capacity (Q_{wt}) is the ratio of the final weight (m_1) after full adsorption to the initial weight (m_0) of GCA as follows:

$$Q_{wt} = \frac{m_1 - m_0}{m_0}$$

To test the adsorption performances over dyes, 17 mg GCA are suspended in 50 mL MB or methyl orange (MO) solution (10 mg/L) with a slight magnetic stirring to maintain the shape of the aerogels. 2 mL of suspension were taken every 1 h and the concentration of dyes was determined on a UV-5100 (Anhui Wanyi) spectrometer.

2.6 Mechanical strength and cyclic adsorption experiment

The mechanical strength test was carried out by the following steps: the obtained GCA was compressed to about 80 % of its own height. After dislodged the compression, the prepared GCA recovered to their original shape quickly. The same process was repeated many times. Two kinds of adsorption cycle experiments were performed. The absorption-distillation and absorption-combustion performances were carried out to evaluate the recycling performances.[7b] For the absorption-combustion experiment, the aerogel was immersed in the organic solvents for about 5 min and then the aerogel was ignited directly in the crucible until the complete combustion of n-hexane, which were repeated for 10 times. For the adsorption-squeezing experiment, n-hexane was dropped on the surface of the aerogels until the adsorbent reached adsorption saturation and then the aerogel was squeezed to half of its height. The same process was repeated 10 times.

3. Results and discussion

3.1 Characterization of GA and GCA

The PXRD patterns of the GO, GA, CNTs and GCA with the GO/CNTs mass ratio of 3:1 are shown in Fig. 1a. A strong diffraction peak at 2θ = 26.1° (*d*-spacing = 3.4 Å) was observed for CNTs, whereas GO exhibited a diffraction peak at 2θ = 9.9° and the corresponding interlayer spacing is 8.9 Å. In addition, a weak peak at 2θ=20.2° was also observed, indicating that the oxygen-containing groups have already been introduced during their oxidation processes.[12] After the reduction process, the peak at 2θ = 9.9° disappeared for GA. Meanwhile, a new broadened diffraction peak at 24.7° (*d*-spacing = 3.7 Å) was observed in GA, which is much lower than that of GO (*d*-spacing = 8.9 Å) but slightly larger than that of natural graphite (3.4 Å), confirming the development of graphitic structures.[16] Moreover, these results revealed the existence of π-π stacking between the graphene sheets in GA, which is composed of inhomogeneously stacked graphene sheets.[7b] In addition, the diffraction patterns of GCA contained the diffraction peaks from both GA and CNTs, pointing out the successful incorporation of CNTs into the GA. Raman spectra of GO, CNTs, GA and GCA (Fig. 1b) display two obvious characteristic peaks at 1335 cm^{-1} and 1590 cm^{-1} corresponding to the D and G bands, respectively, which are due to the defects and disorders of the GO. In addition, a weak band at ca. 2700 cm^{-1} was observed for all the studied samples. This band could be attributed to the two phonon lattice vibrations in the graphitic structure.[15a] The intensity ratio of D and G band (I_D/I_G) in both GA (1.10) and GCA (1.09) are significantly enhanced compared to the GO precursor (1.02), indicating the improvement of disordered graphene sheets.[16] Moreover, the I_D/I_G in GCA (1.09) is larger than that of CNTs (1.06) but smaller than that in GA (1.10), which further demonstrated that the prepared GCA contained both GA and CNTs,[17] matching well with the results from PXRD measurements (Fig. 1a).

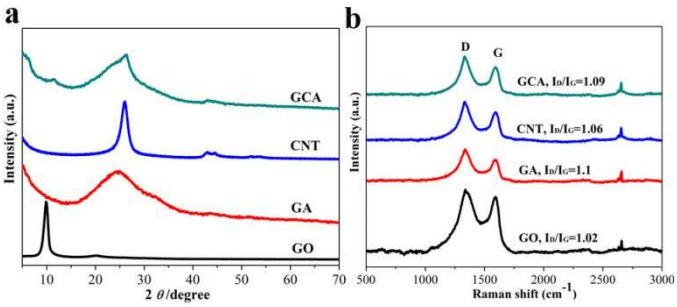

Fig. 1 (a) PXRD patterns and (b) Raman spectra of GO, GA, CNTs and GCA

To understand the effects of different amounts of CNTs on the morphologies of GCA, the samples with GO/CNTs mass ratio of 1:0, 7:1, 3:1 and 5:3 were selected for further investigations. When the GO/CNT ratio is less than 5:3, it was difficult to form hydrogel. The macroscopic structures of these aerogels (Fig. 2a-d) reveal a typical 3D network. The surface of GA was smooth and apparent cracks were observed (Fig. 2a). In the presence of CNTs, no cracks and exfoliation were observed on the surface. Besides, with increasing the amounts of CNTs, the aerogels became more densification (Fig. 2b-d). Meanwhile, the same phenomenon was observed from SEM images (Fig. 2e-h). For pristine GA, most of the graphene sheets were stacked seriously and some large cracks among the stacked layers were observed as well (Fig. 2e). In contrast, the aerogels containing CNTs did not exhibit serious accumulation phenomenon. With increasing the amount of CNTs, graphene sheets became more discrete. Especially, porous structures were appeared with the size of several tens of micrometers and the pore walls consisted of thin layers of a network with cross linked graphene sheets and CNTs (Fig. 2f-h). Nevertheless, when the ratio of GO/CNTs reached to 5:3, the graphene sheets and CNTs suffered different degrees of agglomeration, leading to the destruction of porous structures. Generally, hydrothermal reduction process could promote the form of strong π-π interaction between the graphene sheets due to the restoring of conjugated carbon net. However, in the freeze drying process, some graphene sheets could be separated by the growth force of the ice crystals, resulting in some obvious cracks in the aerogels. Therefore, the freeze drying process has a remarkable impact on the morphology and structure of the final aerogels.[18] For the hybrid aerogels, CNTs played an important role in skeleton and prevented the fragmentation under the same freezing condition. According to the high magnification SEM image (Fig. S1), it was observed that the CNTs in the aerogels play a role as skeleton to maintain the graphene sheets. Furthermore, four kinds of existence

forms between the CNTs and graphene sheets were found (Fig. S2): most of the CNTs are covered on the graphene wall to form net framework (Fig. S2a); some of the CNTs connect two graphene sheets like the sewing thread (Fig. S2b). Apart from these, some CNTs are sandwiched in the middle of graphene sheets (Fig. S2c) and we also observed that the CNTs are wrapped by the graphene sheets (Fig. S2d). Consequently, the multiple existence forms between graphene sheets and CNTs could increase the surface roughness of the sheets, which benefits to form a cross linked structure between layers.

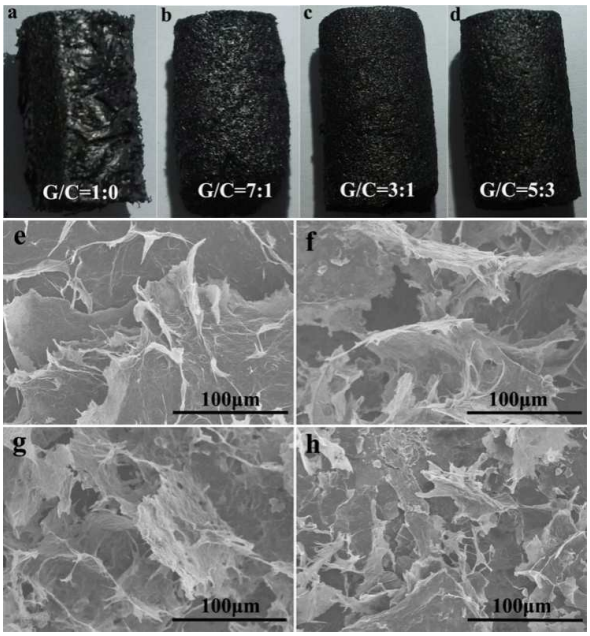

Fig. 2 Photographs of the aerogels with the mass ratio of GO/CNTs (a) 1:0; (b) 7:1 (c) 3:1 (d) 5:3; The corresponding SEM images of the aerogels with the ratio of (a) 1:0; (b) 7:1 (c) 3:1 (d) 5:3.

TEM image of the GCA with GO/CNTs ratio of 3:1 (Fig. S3) reveals the dense and homogeneous distributions of CNTs within the graphene sheets. Higher magnification TEM image (Fig. 3a) further confirms that the CNTs with lengths ranging from several hundreds of nanometres to ten micrometers are tightly adhered on the graphene substrates and are quite flexible. The average diameter of the CNTs is ca. 50 nm. It is worth to note that the CNTs are sandwiched between the graphene sheets observed from the edge of the graphene sheets (marked as circular in Fig. 3a), which is consistent with the observations from SEM (Fig. S2c). High-resolution TEM (HRTEM) image (Fig. 3b) reveals that the obtained GCA has well graphitized structure. Three diffraction rings were observed from the selected area electron diffractions (SAED) pattern (inset in Fig. 3b). The corresponding *d*-spacing of these rings is 3.38 Å, 2.08 Å and 1.22 Å, respectively. All of these results confirmed the crystalline nature of the prepared GCA.

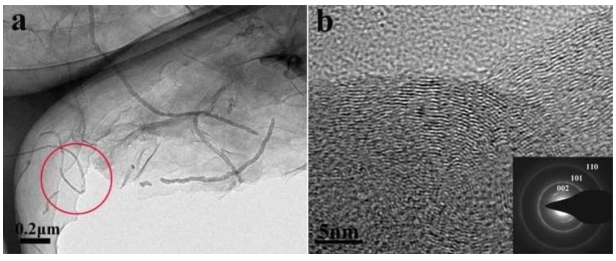

Fig. 3 (a) TEM and (b) HRTEM images of GCA (Inset is the corresponding SAED pattern).

It is well known that CNTs have excellent hydrophobic property. Hence, the incorporation of CNTs in the GA could improve the surface hydrophobicity of GA.[19] As expected, with increasing the amounts of CNTs, the contact angle with water increased from 40° to 114° (Fig. 4a-d). Fig. S4 shows the FT-IR spectra of GO, GA, CNTs and GCA. The graphene synthesized through the reduction of GO by EDA containing hydrophilic functional groups, such as O-H at 3430 cm^{-1}, C-OH at 1389 cm^{-1}, C=O stretching of the carbonyl (COOH) at 1640 cm^{-1}, C-N at 1467 cm^{-1}, which enhanced the interaction between graphene and water. Although the bands of COOH was greatly reduced after reduction from GO to GA, the contact angle of GA is only 40° because the newly formed hydrophilic functional groups such as C-N was introduced during the reduction reaction process. The addition of super hydrophobic CNTs cannot only increase the roughness of the GCA surface (Fig. 2), but also reduce the proportion of GO, leading to a significant improvement of hydrophobicity of GA. In addition, the SSA of GCA with GO/CNTs mass ratio of 1:0, 7:1, 3:1 and 5:3 determined by the MB adsorption method was 84.6 m^2/g, 264.5 m^2/g, 287.1 m^2/g and 127.0 m^2/g, respectively (Fig. 4e). Obviously, the incorporation of CNTs in the GA can also enhance the SSA, which can reach as high as more than 3-fold. Nevertheless, once the ratio of GO/CNTs is higher than that of 3:1, the SSA of GCA decreased, which is in line with the macroscopic structures and SEM observations (Fig. 2).

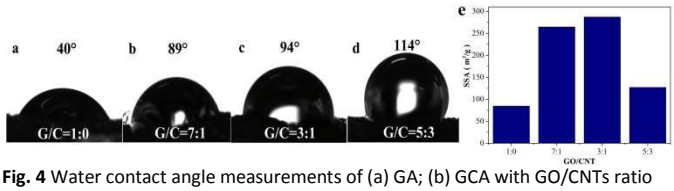

Fig. 4 Water contact angle measurements of (a) GA; (b) GCA with GO/CNTs ratio of 7:1; (c) GCA with GO/CNTs ratio of 3:1; (d) GCA with GO/CNTs ratio of 5:3; (e) SSA of these aerogels.

3.2 The adsorption capacity of GA and GCA

To investigate the selective adsorption properties of the prepared GCA, the oil-water separation experiments using toluene as a target adsorbate were performed. It was observed that the toluene was immediately adsorbed. The completely selective adsorption only took 90 s (Fig. 5a). Moreover, the adsorption experiments using pure oil in the absence of water were carried out to evaluate the effects of CNTs on the Q_{wt} of GA (Fig. 5b). The Q_{wt} of all the aerogels after the incorporation of CNTs increased remarkably compared to the pristine GA no matter of the density of the oils including n-hexane (0.692 g/cm^3), toluene (0.866 g/cm^3), lube (0.910 g/cm^3) and phenixin (1.595 g/cm^3). The Q_{wt} of GA to phenixin and lube can reach ca. 200 and 140 times of its own weight, which are 5-15 times higher than that of the conventional adsorbents such as sponge, active carbon, wool fiber and zeolite.[8] The Q_{wt} of the obtained GCA is not only further enhanced in comparison with GA but is also 3-8 times higher than the previous reported graphene-CNT aerogels.[12]

Among all the aerogels, GCA with GO/CNTs mass ratio of 7:1 and 3:1 exhibit the best adsorption performances and the Q_{wt} for lube and phenixin over these aerogels can reach as high as 190 and 270 g g^{-1}, respectively, which is in line with the SEM observations and SSA measurements (Fig. 2 and Fig. 4). Consequently, SSA is crucial for Q_{wt} instead of contact angle. Not only for the hydrophobic organics, the obtained aerogels can even adsorb the hydrophilic dyes.[20] Fig. 5c and 5d reveal the adsorption curves of two kinds of dyes (MB and MO) for the prepared aerogels. In line with the Q_{wt} measurements, GCA with GO/CNTs mass ratio of 7:1 and 3:1 also exhibited enhanced adsorption to MO and MB compared to other aerogels (Fig. 5c and 5d). Generally, the incorporation of CNTs in GA could promote the formation of micro-porous structures and thus enhance their SSA. Nevertheless, when the GO/CNTs mass ratio reaches to 5:3, the CNTs aggregate severely and the graphene sheets are not sufficient to load-bearing such a large number of CNTs. Hence, the irregular distribution of CNTs and graphene sheets could result in the destruction of porous structures as well as decreasing the SSA. Such porous structure is crucial for the adsorption performance of materials. Because once the oils and organic solvents contact the hydrophobic aerogels, they will penetrate into the aerogels and diffuse in the micro-pores of the aerogels and the pore structure is more conducive to the spread of the oil inside the aerogels. Therefore, the uniform pore cannot only be a diffusion channel, but also wrap the oil inside the aerogels tightly.[15a] However, the orders of the SSA was not entirely consistent with the adsorption capacity. For example, the SSA of the GCA with the ratio of 7:1 was slightly higher than that with the ratio of 3:1, but the Q_{wt} to lube and toluene were even lower. The same phenomenon also happened to the GCA with the ratio of 1:0 and 5:3. This is probably because the adsorption capacity of the aerogels is not only determined by the SSA but also related to the pore size of the aerogels and the nature of the target adsorbates, such as the viscosity and surface tension.[12,15a]

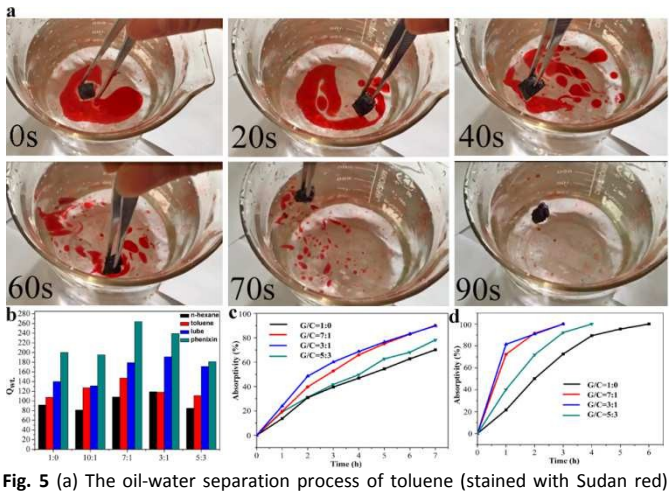

Fig. 5 (a) The oil-water separation process of toluene (stained with Sudan red) from water by the GCA with the mass ratio of 3:1; (b) the Q_{wt} of the GCA with different ratio of GO/CNT (1:0, 10:1, 7:1, 3:1, 5:3). The black, red, blue and green rectangular frames represent the n-hexane, toluene, lube and phenixin, respectively; (c) and (d) the adsorption of the GCA with different ratio of GO/CNT (1:0, 10:1, 7:1, 3:1, 5:3) to MB and MO.

3.3 The reusability and cycling experiments of GA and GCA

The mechanical properties of the aerogels are very important for practical water purification and oil remediation applications. In order to investigate the mechanical properties of the obtained aerogels, the GCA with GO/CNT mass ratio of 1:0 and 3:1 were selected for the mechanical strength measurements. The results have been showed in Movie 1. GCA without CNTs exhibits a poor resilience and the rebound process was accompanied with a hysteresis effect. However, the GCA with the GO/CNT of 3:1 can fleetly rebound in the compression process. This is because the CNTs covered on the graphene sheets could enhance the tenacity of the aerogels. This GCA with CNTs possesses exceptional elastic properties reflected from the compress and rebound experiments, which is in favor of the recyclable performances of aerogels. The treatment of oil leakage not only requires high adsorption efficiency of oil-water separation materials but also needs suitable post-processing. Adsorption-combustion has been considered as a direct and effective way to refresh the oil absorbing materials.[7b] Compared to the traditional adsorptive materials such as polyester sponge and cotton, graphene has very high melting point (over 3000 ^{o}C), which makes graphene aerogels as potential materials for the absorption-combustion process. The sequential images (Fig. 6a-d and Movie 2) show the absorption-combustion process for n-hexane. Remarkably, after combustion, the aerogels could still maintain the 3D structure. In order to investigate the role of CNTs in the aerogels, we also compared the cycling adsorption properties of the GCA (GO/CNTs = 3:1) and GA. According to the absorption-combustion cycling performances (Fig. 6e and 6f), the GA is slightly fragile in comparison with the GCA after several times of combustion and the Q_{wt} decreased about 15% after the first cycle, whereas the GCA is extremely stable and almost no decreasing of Q_{wt} was observed even after 10 cycles. In addition, we further preformed the adsorption-combustion using high viscosity (lube) with the viscosity of 100 mm^2/s (cf. Fig. S5). Due to the high viscosity of the lube, the adsorbed liquids could not flow out from the aerogel glidingly and destroy the aerogel to some extent. The results showed that the adsorption capacity decreased after 10 times of combustion. The aerogel with the ratio of 3:1 had decreased about 33% and the ratio of 1:0 was about 38%. Nevertheless, the GCA aerogel still exhibits an outstanding performance of reusability even adsorbing such a high viscosity organic (Fig. S5).

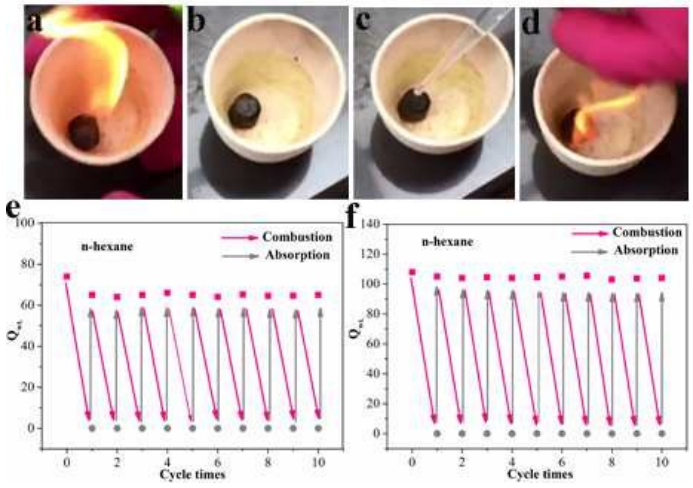

Fig. 6 (a-d) The images of the absorption–combustion process; recyclability of the (a) GA and (f) GCA (GO/CNT=3:1) for the adsorption of n-hexane under absorption–combustion cycles.

Nevertheless, the combustion of oils still causes the environmental pollution and resource wasting. On the basis of the excellent elastic properties (Movie 1), it is expected that the obtained aerogels can collect the oils from the water like the sponge. For this purpose, the adsorption-squeezing experiment was performed.[7b] The images (Fig. 7a-b and Movie 3) demonstrated the cycling performances of our materials. Firstly, n-hexane was dropped on the surface of the aerogels until the adsorbent reached adsorption saturation and then the aerogels were squeezed to half of its height for releasing the organics. Finally, when the aerogels quickly recovered to the original height, the n-hexane was re-dropped on the surface of the aerogels. The mechanical strength of the GCA is good enough and thus almost no reduction of Q_{wt} was observed after ten cycles of squeezing (Fig. 7f), while the GA displayed ca. 13 % decreasing of Q_{wt} after the cycling measurements (Fig. 7e). All in all, our prepared GCA possesses excellent mechanical strength no matter in the air or filled with organics. Hence, GCA exhibited a preferable resistance to the combustion and compression compared with GA.

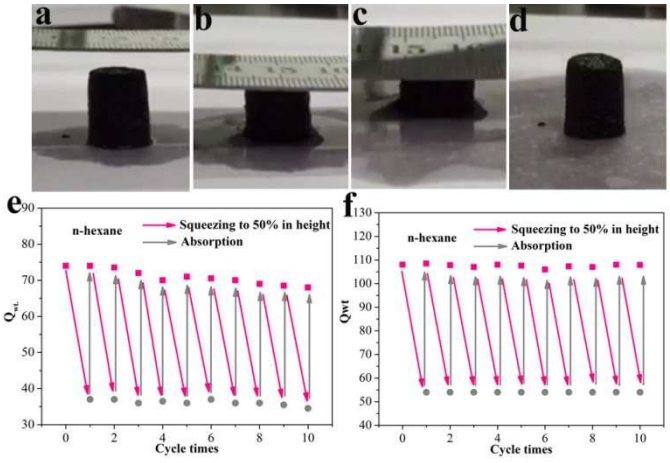

Fig. 7 (a-d) The images of the adsorption-squeezing process; recyclability of the (a) GA and (f) GCA (GO/CNT=3:1) for the absorption of n-hexane under adsorption-squeezing cycles.

4. Conclusions

In summary, ultra-light (6.2-12.8 mg/cm^3) graphene-CNTs aerogels were successfully prepared by a facile hydrothermal method using EDA as a reducing agent. The incorporation of CNTs into GA has significantly influences on the structures, morphologies, SSA, hydrophobic properties, adsorption capacity and mechanical properties of GA. The multiple existence forms of CNTs in graphene sheets could increase the surface roughness of the sheets, thus enhancing the SSA from 84.6 to 287.1 m^2/g. Therefore, the GCA exhibited improved adsorption capacity to oil, organic solvents and dyes compared to GA. When the GO/CNT mass ratios were 7:1 and 3:1, the adsorption capacity can reach 100-270 times of its own weight depending on the density of the adsorbed organics. Importantly, the obtained GCA exhibited excellent reusability and mechanical strength based on the absorption-distillation and absorption-combustion measurements. The GCA can maintain their macroscopic shape and no adsorption capacity decreasing was observed even after 10 cycling experiments, which is very attractive for the practical water purification and oil remediation.

Acknowledgements

Financial support by the Sichuan Youth Science and Technology Foundation (2013JQ0034), the National Natural Science Foundation of China (11405256, U1532120), the Innovative Research Team of Sichuan Provincial Education Department and SWPU (2012XJZT002), and the Open Foundation for the Key Laboratory of Oil and Gas Materials (x151514kcl30) is gratefully acknowledged.

Notes and references

1 (a) J. W. Short, S. D. Rice, R. A. Heintz, M. G. Carls and A. Moles, *Energy Sources*, 2003, **25**, 509; (b) B. Dubansky, A. Whitehead, J. T. Miller, C. D. Rice and F. Galvez, *Environ. Sci. Technol.*, 2013, **47**, 5074.
2 M. Schrope, *Nature*, 2011, **472**, 152.
3 (a) M. O. Adebajo, R. L. Frost, J. T. Kloprogge, O. Carmody and S. Kokot, *J. Porous Mater.*, 2003, **10**, 159; (b) G. Deschamps, H. Caruel, M.-E. Borredon, C. Bonnin and C. Vignoles, *Environ. Sci. Technol.*, 2003, **37**, 1013; (c) H. B. Sonmez and F. Wudl, *Macromolecules*, 2005, **38**, 1623.
4 A. K. Geim, *Science*, 2009, **324**, 1530.
5 Y. X. Xu, Q. Wu, Y. Q. Sun, H. Bai and G. Q. Shi, *ACS Nano.*, 2010, **4**, 7358.
6 M. Toyoda and M. Inagaki, *Spill Sci. Technol. Bull.,* 2007, **8**, 467.
7 (a) M. A. Worsley, P. J. Pauzauskie, T. Y. Olson, J. Biener, J. H. Satcher and Jr., T. F. Baumann, *J. Am. Chem. Soc.*, 2010, **132**, 14067; (b) J. H. Li, J. Y. Li, H. Meng, S. Y. Xie, B. W. Zhang, L. F. Li, H. J. Ma, J. Y. Zhang and M. Yu, *J. Mater. Chem. A,* 2014, **2**, 2934; (c) H. C. Bi, X. Xie, K. B. Yin, Y. L. Zhou, S. Wan, R. S. Ruof and L. T. Sun, *J. Mater. Chem. A.,* 2014, **2**, 1652.
8 (a) Q. Zhu and Q. M. Pan, *ACS Nano.,* 2014, **8**, 1402; (b) A. Bayat, S. F. Aghamiri, A. Moheb and G. R. Vakili-Nezhaad, *Chem. Eng. Technol.*, 2005, **28**, 1525; (c) T. R. Annunciado, T. H. D. Sydenstricker and S. C. Amico, *Mar. Pollut. Bull.,* 2005,

50, 1340 ; (d) M. M. Radetic, D. M. Jocic, P. M. Jovanccic, Z. L. Petrovic and H. F. Thomas, *Environ. Sci. Technol.,* 2003, **37**, 1008.

9 (a) X. C. Gui, J. Q. Wei, K. L. Wang, A. Y. Cao, H. W. Zhu, Y. Jia, Q. K. Shu and D. H. Wu, *Adv. Mater.*, 2010, **22**, 617; (b) H. C. Bi, X. Xie, K. B. Yin, Y. L. Zhou, S. Wan, L. B. He, F. Xu, F. Banhart, L. T. Sun and R. S. Ruoff, *Adv. Funct. Mater.,* 2012, **22**, 4421; (c) S. J. Choi, T. H. Kwon, H. Im, D. IlMoon, D. J. Baek, Myeong-LokSeol, J. P. Duarte and Y. K. Choi, *ACS Appl. Mater. Interfaces.,* 2011, **3**, 4552; (d) N. T. Cervin, C. Aulin, P. T. Larsson and L. Wagberg, Cellulose, 2012, **19**, 401. (e) K. H. Kim, Y. G. Oh and M. F. Islam, *Nature Nanotech.,* 2012, **7**, 562; (e) H. Hu, Z. B. Zhao, W. B. Wan, Y. Gogotsi and J. H. Qiu, *Adv. Mater.*, 2013, **25**, 2219; (f) X. Xie, Y. L. Zhou, H. C. Bi, K. B. Yin, S. Wan and L.T. Sun, *Sci. Rep.,* 2013, 3, 2117.

10 L. Qiu, J. Z. Liu, S. L.Y. Chang, Y. Z. Wu and D. Li, *Nat. Commun.*, 2012 , **3** , 1241.

11 (a) H. Y. Sun , Z. Xu and C, Gao, *Adv. Mater.*, 2013, **25**, 2554; (b) Z. Xu, H. Y. Sun and C. Gao, *APL Mater.,* 2013, 1, 030901;

12 S. Kabiri, D. N. H. Tran, T. Altalhi and D. Losic, *Carbon*, 2014, **80**, 523.

13 (a) Z. Xu , H. Y. Sun, X. L. Zhao and C. Gao, *Adv. Mater.,* 2013, **25**, 188; (b) L. Peng, Y. C. Zheng, J. C. Li, Y. Jin and C. Gao, *ACS Catal.,* 2015, **5**, 3387.

14 X. Li, P. X. Huang, Y. Zhou, H. Peng, W. Li, M. Z. Qu and Z. L. Yu*, Mater. Lett.,* 2014, **133**, 289.

15 (a) D. N. H. Tran, S. Kabiri, T. R. Sim and D. Losic, *Environ. Sci.: Water Res. Technol.*, 2015, **1**, 298. (b) M. Sun, Q. Tang, T. Zhang and G. Wang, RSC Adv., 2014, **4**, 7774; (c) C. Yang, J. Shen, C. Wang, H. Fei, H. Bao and G. Wang, *J. Mater. Chem. A*., 2014, **2**, 1458.

16 W. Chen and L. Yan, *Nanoscale,* 2011, **3**, 3132.

17 Z. Sui, Q. Meng, X. Zhang, R. Ma and B. Cao, *J. Mater. Chem.,* 2012, 22, **18**, 8767.

18 (a) L. Qian and H. F. Zhang, *J. Chem. Technol. Biotechnol.*, 2011, **86**, 172; (b) H. C. Bi, K. B. Yin, X. Xie, Y. L. Zhou, N. Wan, F. Xu, F. Banhart, L. T. Sun and R. S. Ruoff, *Adv. Mater.*, 2012, **24**, 5124.

19 X. C. Dong, J. Chen, Y. W. Ma, J. Wang, M. B. Chan-Park, X. M. Liu, L. Wang, W. Huang and P. Chen, *Chem. Commun.,* 2012**, 48**, 10660.

20 (a) B. Lee, S. Lee, M. Lee, D. H. Jeong, Y. B. Baek, J. Y. Yoon and Y. H. Kim, *Nanoscale*, 2015, **7**, 6782; (b) X. P. Zhang, D. Liu, L. Yang, L. M. Zhou and T. Y. You, *J. Mater. Chem. A*, 2015, **3**, 10031.